

Influence of Projectile Breakup on Fusion with ^{159}Tb Target; Measurement of CF and ICF cross sections

M.K. Pradhan¹

*Nuclear Physics Division, Saha Institute of Nuclear Physics
1/AF Bidhannagar, Kolkata-700064, India
E-mail: mukeshk.pradhan@saha.ac.in*

A. Mukherjee, P. Basu, A. Goswami, R. Kshetri, S. Roy, P. Roy Chowdhury, M. Saha Sarkar

*Nuclear Physics Division, Saha Institute of Nuclear Physics
1/AF Bidhannagar, Kolkata-700064, India*

R. Palit

Dept. of Nuclear & Atomic Physics, Tata Institute of Fundamental Research, Mumbai-400005, India

V.V. Parkar, S. Santra

Nuclear Physics Division, Bhabha Atomic Research Centre, Mumbai-400085, India

To study projectile breakup effects on fusion reactions with ^{159}Tb target, the measurements of complete fusion (CF) cross sections for the $^{11}\text{B}+^{159}\text{Tb}$, $^{10}\text{B}+^{159}\text{Tb}$, $^7\text{Li}+^{159}\text{Tb}$ and $^6\text{Li}+^{159}\text{Tb}$ reactions at energies around their respective Coulomb barriers are highly desirable. The four reactions, in fact, show that at below-barrier energies, the measured CF cross sections are enhanced compared to the predictions of the 1D BPM calculations and at above-barrier energies for the $^{10}\text{B}+^{159}\text{Tb}$, $^7\text{Li}+^{159}\text{Tb}$ and $^6\text{Li}+^{159}\text{Tb}$ reactions, CF cross sections are suppressed by projectile breakup effects with respect to the coupled channels (CC) calculations. The CF cross section suppression effects are correlated with the α -breakup threshold of the projectiles. Also, the measured incomplete fusion (ICF) cross sections for the $^{10}\text{B}+^{159}\text{Tb}$, $^7\text{Li}+^{159}\text{Tb}$ and $^6\text{Li}+^{159}\text{Tb}$ reactions show that the ICF process, with α -emitting channel, is the dominant contributor and this observation is found to be consistent with the Q-values of the reactions.

*VI European Summer School on Experimental Nuclear Astrophysics
Acrireale Italy
September 18-27, 2011*

¹ Speaker

Introduction

A great interest has been devoted in investigating the fusion process between two heavy ions at energies around the Coulomb barrier, mainly to understand the reaction mechanisms and also to understand the effect of structure of colliding nuclei and transfer of nucleon(s), if any [1,2]. The one-dimensional barrier penetration model (1D BPM), one of the simplest model for describing the fusion process, gives a reasonably agreement with the measured fusion cross sections at energies around the barrier for fusion of light nuclei. However, for heavy-nuclei fusion at below-barrier energies, the measured cross sections are observed to be enhanced by several orders of magnitudes when compared to the 1D BPM calculations. This sub-barrier fusion enhancement is explained to be due to the effect of coupling of the elastic channel to the intrinsic degrees of freedom such as deformation, collective excitation, transfer of nucleons *etc.* and at present this subject is reasonably well understood [2]. However in case of reactions involving weakly bound projectiles (*e.g.*, ^6He , ^{11}Be , ^{11}Li , ^9Be , ^7Li , ^6Li which have breakup threshold energies less than 1 MeV to a few MeV), owing to the very low binding energies, the weakly bound projectile may breakup in the field of the target nucleus and hence may influence the fusion process.

Over the past few years, there have been a great interest in investigating the effect of breakup of weakly bound nuclei on fusion. Although there have been many experimental and theoretical works on this subject, it is still far from being fully understood [3]. There is a special interest in this study because of the recent increasing availability of beams of loosely bound radioactive nuclei. The interest is focused on understanding the structure of halo unstable nuclei and to investigate the effect of their unusual properties (like halo/skin and large breakup probability) on the reaction mechanisms. Study of some of the reactions involving unstable nuclei have great implications in the field of nuclear astrophysics and also in the search of mechanisms for producing superheavy nuclei.

Till date, the available beams of unstable nuclei have very low intensity and also have poor beam energy resolution. For this reason, precise measurement of fusion cross sections involving such nuclei is difficult, though some results is already available [3]. On the other hand, precise measurement of fusion cross sections is possible with stable weakly bound nuclei (^6Li , ^7Li , ^9Be) having sufficiently low breakup thresholds and which are produced easily with high intensity. In fusion with such stable nuclei, most of the essential features of breakup can be studied, though some of the unusual properties that halo unstable nuclei exhibit are absent. Therefore, a full understanding of the reaction mechanisms of such stable weakly bound nuclei with targets of masses varying from heavy, medium to light and covering the energy region from well below to well above the Coulomb barrier may serve as an important reference for understanding similar studies of reactions involving light unstable nuclei.

The breakup process of a weakly bound projectile gives rise to different kinds of fusion: (i) the usual complete fusion (CF), where the whole projectile fuses with the target to form the compound nuclei, (ii) the incomplete fusion (ICF), where the projectile breaks up and subsequently one of the fragments is absorbed by the target while the other escapes the interaction region. From literature survey, one finds that for light and medium mass systems,

like, $^{6,7}\text{Li}+^{12,13}\text{C}$, $^{6,7}\text{Li}+^{16}\text{O}$, $^{6,7}\text{Li}+^{59}\text{Co}$, $^9\text{Be}+^{64}\text{Zn}$ *etc.* [3], owing to experimental limitations, separation of CF and ICF events were not possible, and so only the total fusion (TF = CF+ICF) cross sections were measured. It was observed that there is no effect of breakup on TF at energies around the Coulomb barrier. However, for heavy mass systems, like, $^{6,7}\text{Li}+^{209}\text{Bi}$, $^9\text{Be}+^{208}\text{Pb}$ *etc.* [3], experimentally it is possible to measure CF and ICF cross sections separately. For such systems, it was observed that at above-barrier energies, CF cross sections are suppressed by around 30% with respect to the coupled channels (CC) calculations [3].

In this context, it is interesting to see what happens in the mass region between the medium and heavy mass region. So, we chose to study the mass region $A \sim 160-170$. In order to investigate the effect of breakup on fusion, the reactions studied with weakly bound nuclei are usually performed using ^6Li , ^7Li and ^9Be that have α -breakup threshold energies from 1.47 to 2.45 MeV. However, among the stable weakly bound nuclei, apart from ^6Li , ^7Li and ^9Be , the nucleus ^{10}B also has a relatively low α -separation energy of 4.5 MeV. Therefore like ^6Li , ^7Li and ^9Be , the nucleus ^{10}B is also expected to break up at considerably low bombarding energy and hence it may influence the fusion process. So to investigate the influence of α -breakup threshold on fusion, the systems $^{11}\text{B}+^{159}\text{Tb}$, $^{10}\text{B}+^{159}\text{Tb}$, $^7\text{Li}+^{159}\text{Tb}$ and $^6\text{Li}+^{159}\text{Tb}$ have been studied at energies around the respective Coulomb barriers, where $^{11}\text{B}+^{159}\text{Tb}$ has been chosen as the reference strongly bound system, because the nucleus ^{11}B having α -separation energy of 8.66 MeV, is comparatively strongly bound among the four projectiles considered in our work.

Experimental Details & Results

The experimental study has been performed at the 14UD BARC-TIFR Pelletron accelerator at TIFR, Mumbai by using $^{11,10}\text{B}$ beams, with energies in the range 38-72 MeV, and $^{7,6}\text{Li}$ beams with energies in the range 23-43 MeV. The beams, accelerated by the Pelletron, bombarded a self-supporting ^{159}Tb foil of thickness of $1.50 \pm 0.07 \text{ mg/cm}^2$ ($1.59 \pm 0.08 \text{ mg/cm}^2$ for $^6\text{Li}+^{159}\text{Tb}$ measurement). Fusion cross section measurements of the three systems $^{11}\text{B}+^{159}\text{Tb}$, $^{10}\text{B}+^{159}\text{Tb}$ and $^7\text{Li}+^{159}\text{Tb}$ were performed in a single run, while the measurement of the $^6\text{Li}+^{159}\text{Tb}$ reaction was performed in a separate run. During the run for the $^6\text{Li}+^{159}\text{Tb}$ reaction, measurements for the $^7\text{Li}+^{159}\text{Tb}$ reaction at a few energies were also repeated to check the consistency of the results between the two runs. The emitted γ -rays were detected in a Compton suppressed clover detector placed at $+55^\circ$ ($+125^\circ$ for $^6\text{Li}+^{159}\text{Tb}$ run) with respect to the incident beam direction. In both runs, two $300 \mu\text{m}$ thick Si-surface barrier detectors were placed inside the reaction chamber at angles $\pm 30^\circ$ with respect to the incident beam axis to allow the normalization of the data and the beam monitoring as well. The absolute full energy peak detection efficiency of each of the γ -ray detectors was determined by using the calibrated standard radioactive sources (^{152}Eu , ^{133}Ba , ^{207}Bi , ^{60}Co , ^{137}Cs) placed at the same geometry as that for the target. Both in-beam spectra and off-beam decay spectra were taken for each of the bombarding energies. The total charge of each beam exposure was measured using a 1 m long Faraday cup placed after the target and from that the number of incident beam particles was determined. The target thickness was determined using the different techniques: i) the energy loss method, ii) the Rutherford scattering method, and from iii) the $137.5 \text{ keV } [7/2^+ \rightarrow 3/2^+ (\text{g.s.})]$

Coulomb excitation line of ^{159}Tb nucleus. The thickness of the target obtained from three different methods had good agreement, within 5%.

The compound nuclei ^{170}Yb , ^{169}Yb , ^{166}Er and ^{165}Er , formed in the fusion process $^{11}\text{B}+^{159}\text{Tb}$, $^{10}\text{B}+^{159}\text{Tb}$, $^7\text{Li}+^{159}\text{Tb}$ and $^6\text{Li}+^{159}\text{Tb}$ respectively, decay predominantly by neutron evaporation. This is also predicted by the statistical model calculations performed by using the PACE2 code [4]. From an experimental point of view, it is possible to distinguish the evaporation residues (ERs) produced following the CF process from those produced in the ICF process, as discussed in Ref. [3]. We mention that in the energy range investigated here, fission is unimportant for these reactions. Therefore the CF cross sections were obtained from the sum of the cross sections of the ERs produced following xn evaporation of the compound nuclei. In case of the $^{11}\text{B}+^{159}\text{Tb}$ and $^{10}\text{B}+^{159}\text{Tb}$ reactions, an evaporation of neutrons (three to six) occurs, resulting in the formation of $^{167-164}\text{Yb}$ and $^{166-163}\text{Yb}$ ERs, respectively. In the case of the $^7\text{Li}+^{159}\text{Tb}$ and $^6\text{Li}+^{159}\text{Tb}$ reactions, the evaporation of two or five neutrons produces the ERs $^{164-161}\text{Er}$ and $^{163-160}\text{Er}$, respectively. All the previous arguments refer to the energy range investigated here.

In order to determine the cross sections of the ERs, the online spectra were used. In the in-beam method, the cross sections of the even-even ERs were obtained by measuring the γ -ray cross sections, $\sigma_\gamma(J)$, for the various transitions in the ground-state rotational band of the relevant nucleus and then extrapolating it to ground state spin $J^\pi=0^+$. But for the odd-mass nuclei, the level schemes are not simple like the even-even nuclei, and so their cross sections were obtained by summing the measured cross sections of the prompt γ -rays that feed the ground state of the nuclei. Whenever possible, the cross sections of some of the odd-mass nuclei were also measured by the off-beam method, following the respective radioactive decay. Cross sections obtained using the two methods in such cases were found to be in good agreement, thereby showing that the ground state contributions are not significant. It should be mentioned that in determining the γ -ray cross sections, corrections for the internal conversion were appropriately included. The measured CF excitation functions for the four systems thus obtained are shown in Figs. 1(a-d).

To compare the measured CF cross sections with the theoretical calculations, 1D BPM was used to calculate the fusion cross sections. The calculation was done using the realistic coupled channels (CC) code CCFULL [5], in the no coupling limit. The bare potential used in the calculations was the Woods-Saxon parameterization of the Akyüz-Winther (AW) potential [6]. The CCFULL calculations with the shallow potentials lead to oscillations in the transmission coefficients of high partial waves, especially at high energies. To minimize such oscillations, the potential wells for the four systems were chosen to be sufficiently deep so that the ingoing-wave boundary condition (IWBC) is correctly applied. The diffuseness parameter was chosen to be at $a = 0.85 \text{ fm}$ for all the four systems, following the systematic trend of high diffuseness parameter required to fit the high energy part of the fusion excitation functions [7]. Then the depth (V_0) and radius parameters (r_0) were varied so that the corresponding 1D BPM cross sections agree with those calculated using the AW potential parameters at higher energies. The results of 1D BPM calculations are shown by the dash-dot-dot lines in Figs. 1(a-d). We observed that for all the four reactions, the measured CF cross sections are enhanced at below-barrier energies compared to the predictions of 1D BPM calculations. However, for $^{11}\text{B}+^{159}\text{Tb}$,

at above-barrier energies, the 1D BPM calculations reproduce the measured CF cross sections, but for $^{10}\text{B}+^{159}\text{Tb}$, $^7\text{Li}+^{159}\text{Tb}$ and $^6\text{Li}+^{159}\text{Tb}$, the measured CF cross sections are found to lie well below the 1D BPM calculations. So, at above-barrier energies, the measured CF cross sections for $^{10}\text{B}+^{159}\text{Tb}$, $^7\text{Li}+^{159}\text{Tb}$ and $^6\text{Li}+^{159}\text{Tb}$ reactions are suppressed compared to the 1D BPM calculations.

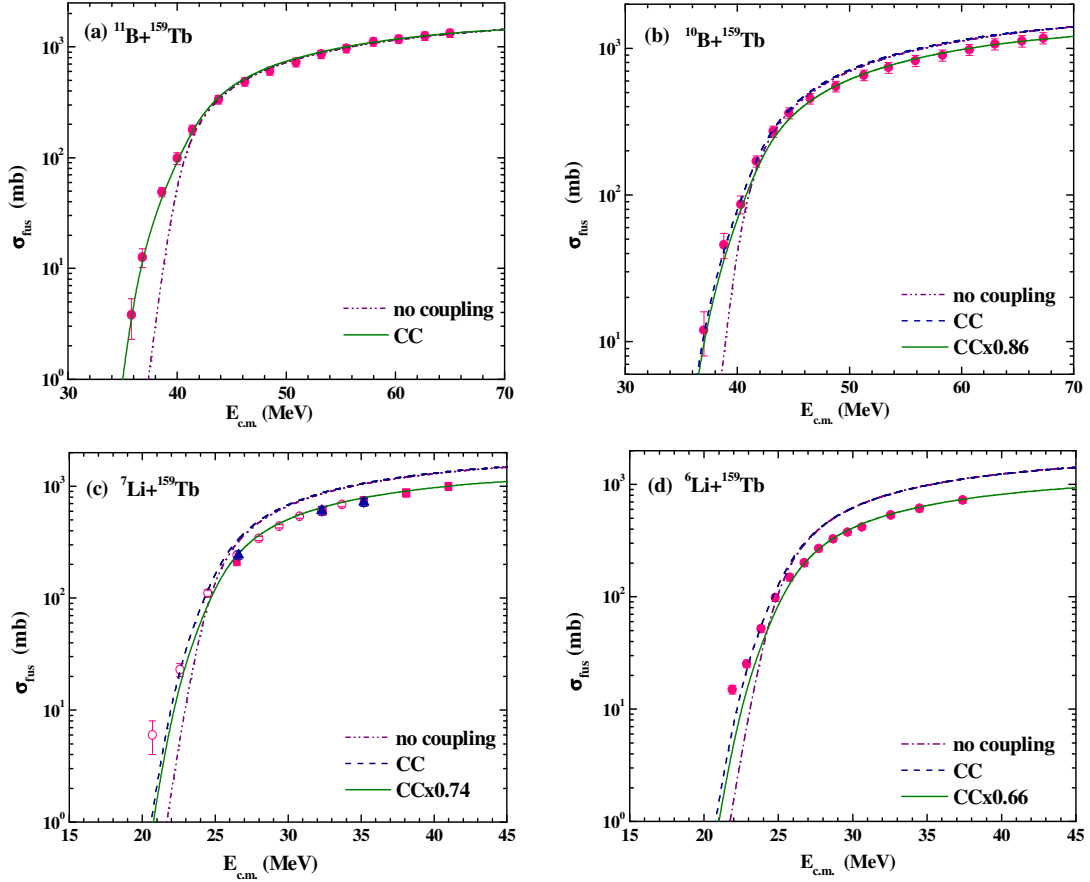


Fig. 1. Complete fusion (CF) cross sections as a function of centre-of-mass energy for the $^{11}\text{B}+^{159}\text{Tb}$, $^{10}\text{B}+^{159}\text{Tb}$, $^7\text{Li}+^{159}\text{Tb}$ and $^6\text{Li}+^{159}\text{Tb}$ reactions. The hollow points in $^7\text{Li}+^{159}\text{Tb}$ are taken from the measurements of Broda *et al.* [8]. The solid triangles in $^7\text{Li}+^{159}\text{Tb}$ show the results obtained from the present work taken during the $^6\text{Li}+^{159}\text{Tb}$ run. The dash-dot-dot line shows the 1D BPM calculations. The dashed line (solid line in $^{11}\text{B}+^{159}\text{Tb}$) represents the CC calculations. The solid line in $^{10}\text{B}+^{159}\text{Tb}$, $^7\text{Li}+^{159}\text{Tb}$ and $^6\text{Li}+^{159}\text{Tb}$ shows the CC calculations when multiplied by the factor 0.86, 0.74, and 0.66 respectively.

To study the effect of coupling and also the extent of CF suppression at above barrier energies in a theoretical framework, the coupled channels (CC) calculations were performed using the same code CCFULL to calculate the fusion cross sections. The enhancement of CF cross sections at below-barrier energies for all the four systems could be due to the effect of target deformation (^{159}Tb is a well deformed nucleus). The CC calculations were done by including the excited states of the target only. The excitation of the target is described within a rotational model by deforming the potentials with deformation parameters $\beta_2=0.344$ [9] and $\beta_4=0.062$ [10]. The CC calculations for the $^{11}\text{B}+^{159}\text{Tb}$ system are shown by the solid line in Fig.

1(a) and those for the $^{10}\text{B}+^{159}\text{Tb}$, $^7\text{Li}+^{159}\text{Tb}$, $^6\text{Li}+^{159}\text{Tb}$ systems are shown by the dashed lines in Figs. 1(b-d). The CC calculated fusion cross sections are found to be in good agreement with the measured CF cross sections for the $^{11}\text{B}+^{159}\text{Tb}$ reaction. However, for $^{10}\text{B}+^{159}\text{Tb}$, $^7\text{Li}+^{159}\text{Tb}$ and $^6\text{Li}+^{159}\text{Tb}$ reactions, at below-barrier energies though the CC calculations well agree with the measured CF cross sections, at above-barrier energies the measured CF cross sections lie well below the CC calculations. The agreements of the CC calculations with the measured CF cross sections at below-barrier energies for all the four systems, shows that the sub-barrier fusion enhancement is primarily due to the effect of target deformation. The small difference, that can be seen at the lowest energy for the $^7\text{Li}+^{159}\text{Tb}$ and $^6\text{Li}+^{159}\text{Tb}$ reactions, could be due to the projectile deformation effect and/ or projectile breakup effect, which could not be considered here. So at above-barrier energies, where coupling is not expected to play any significant role, the CF cross sections are found to be suppressed compared to the CC calculations. As the CC model cannot yet separate the CF and ICF events, the measured CF cross sections could only be compared with the calculated total fusion (TF) cross sections. In order to have an estimate of the extent of the CF suppression with respect to the TF cross sections, the CC calculations for the $^{10}\text{B}+^{159}\text{Tb}$, $^7\text{Li}+^{159}\text{Tb}$ and $^6\text{Li}+^{159}\text{Tb}$ reactions, were scaled by factors of 0.86, 0.74 and 0.66 respectively, to reproduce the high energy part of the measured CF cross sections. The resulting scaled calculations are shown by solid lines in the Figs. 1(b-d). Thus the CF suppression for the three systems $^{10}\text{B}+^{159}\text{Tb}$, $^7\text{Li}+^{159}\text{Tb}$ and $^6\text{Li}+^{159}\text{Tb}$ obtained are $14\pm 5\%$, $26\pm 5\%$ and $34\pm 5\%$ respectively, where an uncertainty of $\sim 5\%$ has been estimated resulting from the overall errors in the measured CF cross sections. If we try to correlate the CF suppression with the α -breakup threshold of the projectiles ($Q_\alpha = -8.66, -4.5, -2.45$ and -1.47 MeV for ^{11}B , ^{10}B , ^7Li and ^6Li respectively), we find that the lower is the α -breakup threshold of the projectile, the higher is the extent of CF suppression, *i.e.*, the extent of CF suppression is correlated with the α -breakup threshold of the projectile. This above-barrier CF suppression is attributed to be due to the loss of flux from the fusion channel caused by breakup of the weakly bound projectiles ^{10}B , ^7Li and ^6Li and hence a major part of this suppression should be going into the ICF channels.

In order to have a complete picture of the fusion process in a reaction, apart from the measurement of CF cross sections, it is also very important to measure the ICF cross sections. In addition to the γ -rays corresponding to the residual nuclei produced following the CF process, the γ -ray spectra of the $^{10}\text{B}+^{159}\text{Tb}$, $^7\text{Li}+^{159}\text{Tb}$ and $^6\text{Li}+^{159}\text{Tb}$ reactions also show the γ -rays corresponding to the product nuclei following the ICF process. For the $^{11}\text{B}+^{159}\text{Tb}$, no γ -rays following any ICF process were observed in the spectra over the energy range of present measurement. In the $^7\text{Li}+^{159}\text{Tb}$ and $^6\text{Li}+^{159}\text{Tb}$ reactions, the γ -rays corresponding to the Dy and Ho isotopes were observed in the spectra. For the $^{10}\text{B}+^{159}\text{Tb}$ reaction, the γ -rays corresponding to the Er isotopes were observed in the spectra. In the $^7\text{Li}+^{159}\text{Tb}$ and $^6\text{Li}+^{159}\text{Tb}$ reactions, the Dy isotopes are produced by the capture of lighter projectile fragment t and d following the breakup of ^7Li and ^6Li respectively by the target ^{159}Tb and subsequent emission of neutrons. Similarly, Ho isotopes are produced by capture of heavier fragment α by ^{159}Tb target and subsequent evaporation of neutrons. For the $^{10}\text{B}+^{159}\text{Tb}$ reaction, the Er isotopes are produced by the capture of heavier fragment ^6Li following the breakup of ^{10}B , by the target ^{159}Tb and subsequent neutron

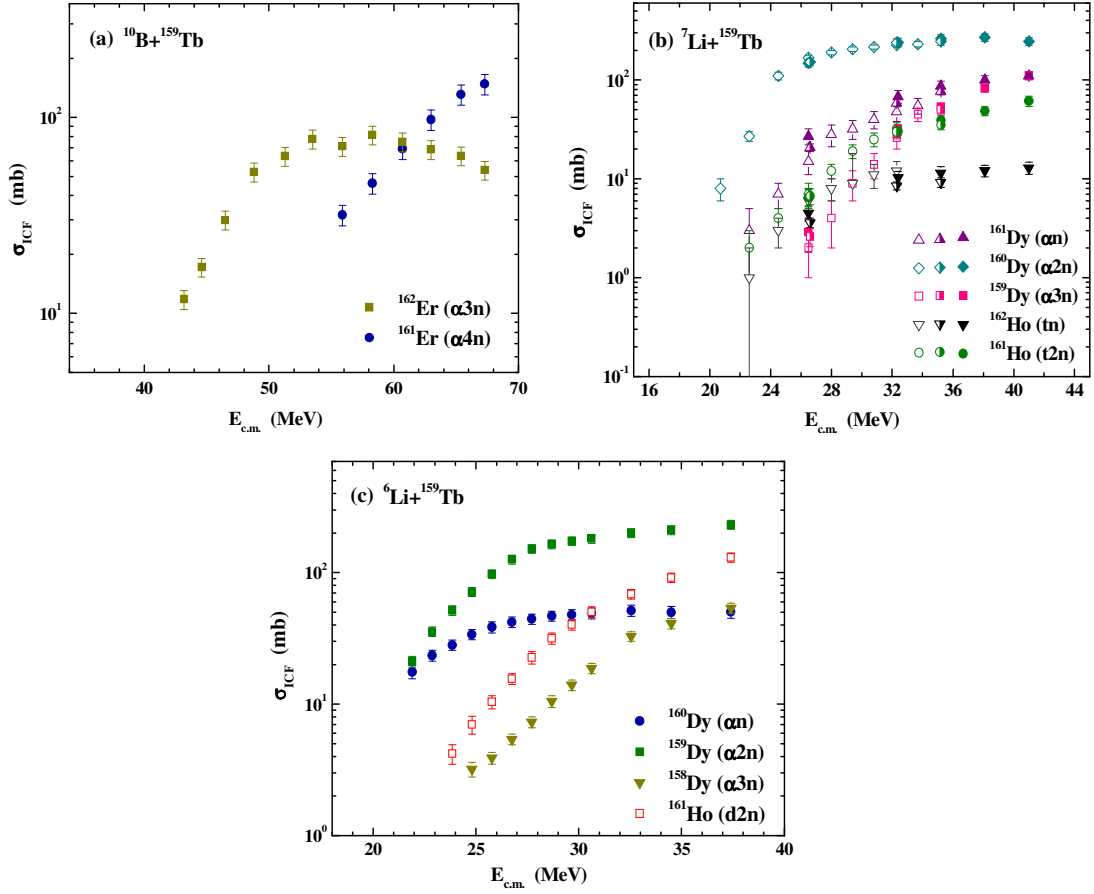


Fig. 2. The ICF channel cross sections as a function of the centre-of-mass energies for the $^{10}\text{B}+^{159}\text{Tb}$, $^7\text{Li}+^{159}\text{Tb}$ and $^6\text{Li}+^{159}\text{Tb}$ reactions. The data corresponding to hollow points in $^7\text{Li}+^{159}\text{Tb}$ are taken from the measurement of Broda *et al* [8]. The half-filled points in $^7\text{Li}+^{159}\text{Tb}$ show the results obtained from the present work taken during the run for $^6\text{Li}+^{159}\text{Tb}$ reaction.

evaporation. The cross sections of the ICF products are determined in a similar way as that for the CF products and are shown in the Figs. 2(a-c). We mention here that the cross sections of the ICF products shown in the Fig. 2 also include contributions due to the direct transfer from projectile to the higher excited states of the target, if any is present, since in the present γ -ray measurement it is not possible to distinguish between the ICF process and direct transfer. From the Fig. 2, we observe that the ICF process with α -emitting channel is the dominant process. If we try to explain this observation by considering the Coulomb barrier, then we find that Coulomb barrier argument holds for $^7\text{Li}+^{159}\text{Tb}$ and $^6\text{Li}+^{159}\text{Tb}$ reactions but not for the $^{10}\text{B}+^{159}\text{Tb}$ reaction. However, if we consider the Q-values of the reactions, then we find that for $^7\text{Li}+^{159}\text{Tb}$ and $^6\text{Li}+^{159}\text{Tb}$ reactions, Q-value corresponding to the capture of lighter fragment (t and d) is positive (+11.1 MeV and +10.2 MeV), whereas it is negative (-3.2 MeV and -2.2 MeV) corresponding to the capture of heavier fragment (α). On the other hand, for the $^{10}\text{B}+^{159}\text{Tb}$ reaction, the Q-value corresponding to the capture of heavier fragment (^6Li) is positive (+4.6 MeV), whereas it is negative (-5.2 MeV) for the capture of lighter fragment (α). So the

observation that ICF with α -emitting channel is the dominant process is consistent with the Q-values of the reactions.

Summary & Conclusions

We have measured the CF cross sections for the four reactions $^{11}\text{B}+^{159}\text{Tb}$, $^{10}\text{B}+^{159}\text{Tb}$, $^7\text{Li}+^{159}\text{Tb}$ and $^6\text{Li}+^{159}\text{Tb}$ at energies around their respective Coulomb barrier. At below-barrier energies, an enhancement of CF cross sections, with respect to the 1D BPM calculations, was observed for the four reactions and this was explained primarily as the effect of target deformation. At above-barrier energies, for the three reactions $^{10}\text{B}+^{159}\text{Tb}$, $^7\text{Li}+^{159}\text{Tb}$ and $^6\text{Li}+^{159}\text{Tb}$, the measured CF cross sections are found to be suppressed, compared to the CC calculations, by $14\pm 5\%$, $26\pm 5\%$ and $34\pm 5\%$ respectively. The extent of CF suppression is found to be correlated with the α -breakup threshold of the projectiles. This above-barrier suppression is attributed due to the loss of flux caused by breakup of the projectiles in the incident channel. We have also measured the ICF channel cross sections for the three reactions $^{10}\text{B}+^{159}\text{Tb}$, $^7\text{Li}+^{159}\text{Tb}$ and $^6\text{Li}+^{159}\text{Tb}$. We found that for all these reactions, the ICF process with α -emitting channel is the dominant contributor and this observation is found to be consistent with the Q-values of the reactions.

Acknowledgments

We are grateful to Professor B. Dasmahapatra for valuable discussions and advice at various stages of the work. We thank P.K. Das for his earnest technical help during the experiment. We would also like to thank the accelerator staff at the BARC-TIFR Pelletron Accelerator Facility, Mumbai, for their untiring efforts in delivering the beams.

References

- [1] M. Beckerman, *Phys. Rep.* **129**, 145 (1985); *Rep. Prog. Phys.* **51**, 1047 (1988)
- [2] M Dasgupta *et al.*, *Ann. Rev. Nucl. Part. Sci.* **48**, 401 (1998)
- [3] L.F. Canto *et al.*, *Phys. Rep.* **424**, 1 (2006), and references therein
- [4] A. Gavron, *Phys. Rev. C* **21**, 230 (1980)
- [5] K. Hagino *et al.*, *Comput. Phys. Commun.* **123**, 143 (1999)
- [6] R.A. Broglia, A. Winther, *Heavy Ion Reactions*, Vol. 1, Benjamin/Cummings, MA, 1981
- [7] J.O. Newton *et al.*, *Phys. Lett. B* **586**, 219 (2004)
- [8] R. Broda *et al.*, *Nucl. Phys. A* **248**, 356 (1975)
- [9] S. Raman *et al.*, *At. Data Nucl. Data Tables* **36**, 1 (1987)
- [10] P. Möller *et al.* *At. Data Nucl. Data Tables* **59**, 185 (1995)